Opportunities in Angularly Resolved Dark-field STEM using Fast Pixelated Detectors

Lewys Jones*[1], Hao Yang[1], Katherine E. MacArthur[1], Henning Ryll[2], Martin Simson[3], Heike Soltau[3], Yukihito Kondo[4], Ryusuke Sagawa[4], Hiroyuki Banba[4], and Peter D. Nellist[1]

1. Department of Materials, University of Oxford, Oxford, UK
2. PNSensor GmbH, Otto-Hahn-Ring 6, 81739 München, Germany
3. PNDetector GmbH, Sckellstraße 3, 81667 München, Germany
4. JEOL Ltd.,3-1-2 Musashino Akishima Tokyo 196-8558 Japan

Background

The aberration corrected scanning transmission electron microscope (STEM) is able to probe materials down to the atomic scale. Often images are created using either small on-axis detectors (bright-field) or large annular detectors with a fixed size (dark-field). However, far more information is available in the diffraction plane than these simple detectors record (Figure 1). By using a pixelated detector (camera) the entire diffraction pattern can be recorded for every probe position yielding a four-dimensional dataset [1]. Once acquired, any number of virtual detectors can be created and images synthesised without the need for pre-configured fixed detector angles [2].

Recording speeds are however slower than conventional STEM detectors with the examples shown in Figures 3 and 5 having 256x256 real-space probe positions recorded at 1000 diffraction patterns per second (264x264 camera pixels, ≈65s total recording time).

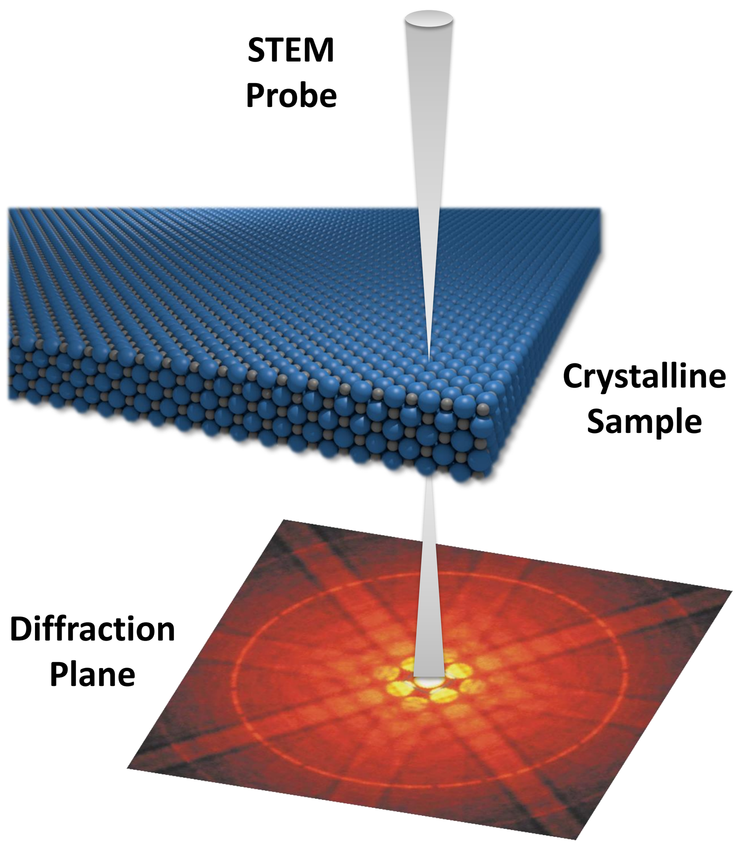

Figure 1. Schematic of focused probe illumination in the STEM and the resulting diffraction pattern. The rich information in the diffraction plane includes diffracted disks, Kikuchi bands, the HOLZ ring and a background contribution from thermal diffuse scattering.

Hardware Setup on JEOL 200CF

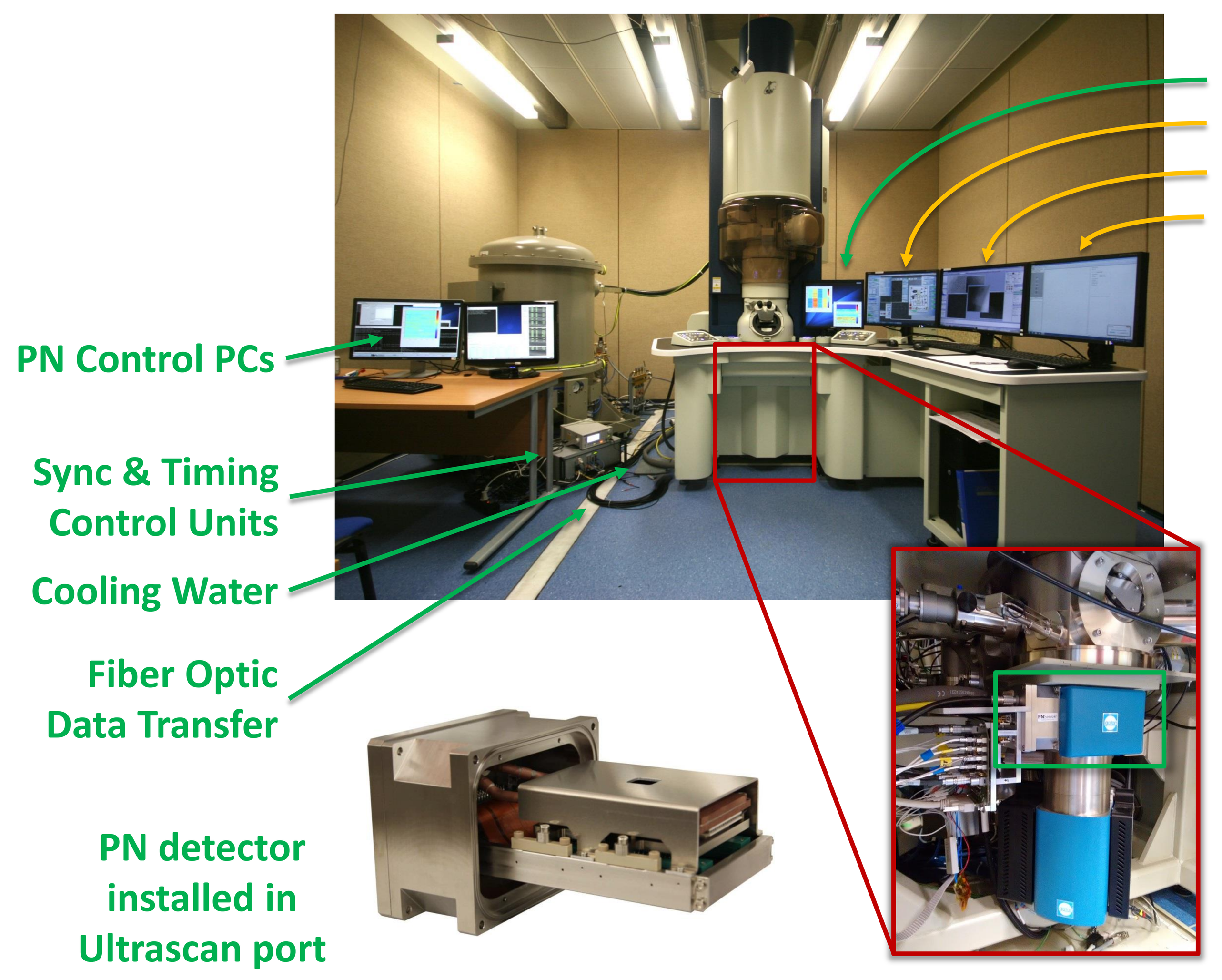

Figure 2. *Installation of PN detector system on a JEOL 200CF.*

Sensor is installed in the Ultrascan port below the viewing screen above the GIF.

Data is transferred to a sever rack by fiber optic cable and the chip is cooled using a closed-loop chilled water circuit.

An additional workstation is setup for the camera operator with a live view of the sensor image relayed to an additional monitor positioned for the microscope operator.

Synthesising BF, ABF, ADF & PACBED

By separating the processes of data-acquisition and image formation, the 4D data-block can be evaluated interactively to optimise the synthetic-detector geometry. Figure 3 shows some of the example images that can all be synthesised from the same experimental scan.

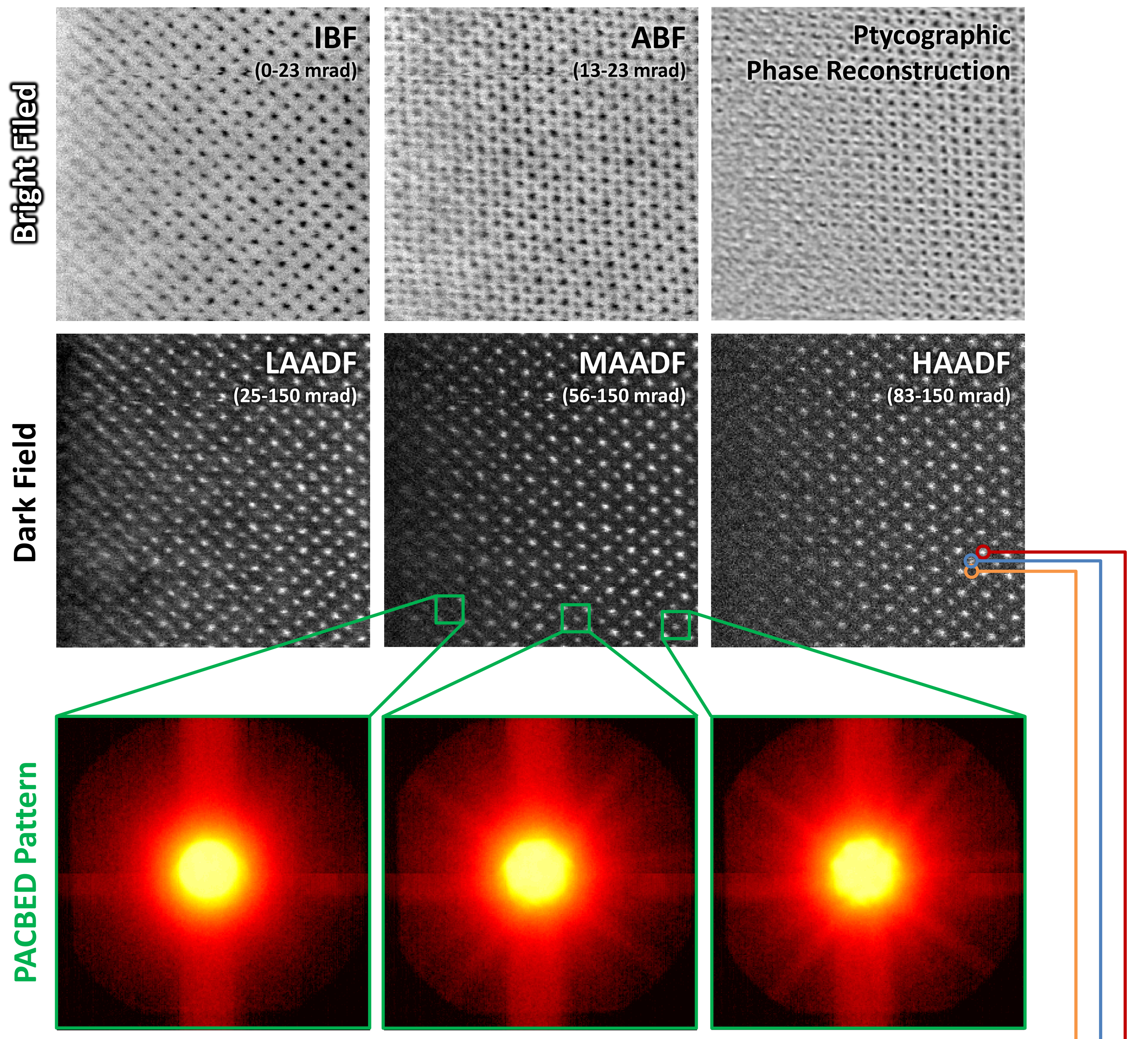

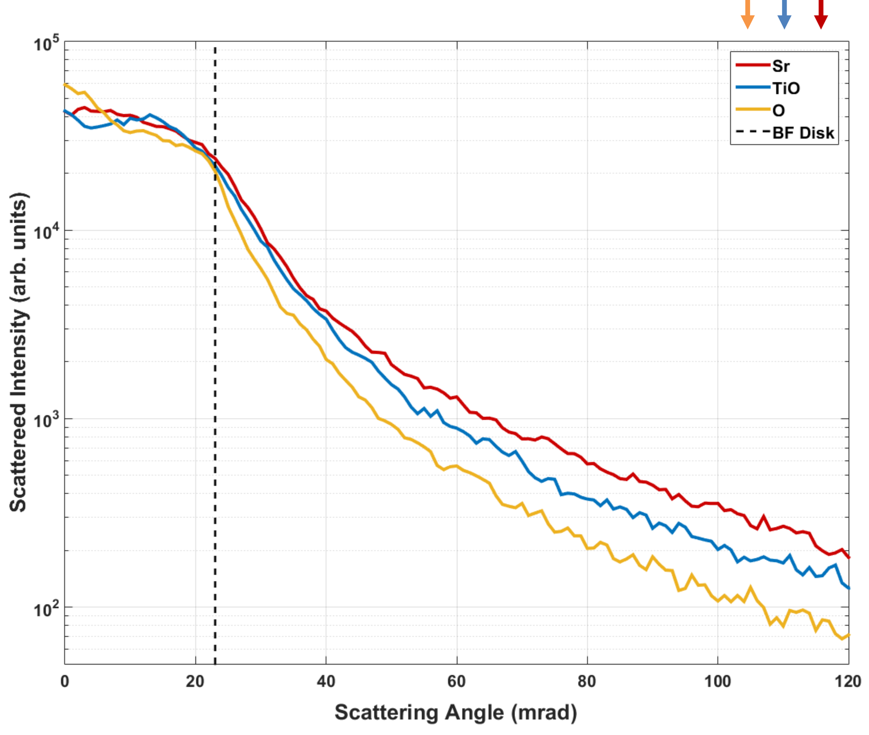

Figure 3. *Examples of the possible images that can be reconstructed using different synthetic detectors or modes. The sample is a [100] oriented $SrTiO_3$ wedge with thickness increasing from left to right. The panels above show incoherent bright-field (IBF), annular bright-field (ABF), and low-, medium-, and high-angle annular dark-filed images.*

The IBF image shows clearly the metal containing columns, while ABF also shows the oxygen column positions. The transmission function phase (as retrieved by ptycography [3]) is also shown for comparison; this has a higher resolution but shows defocus/propagation effects.

The LAADF images shows atomic columns on the left edge (thin region) clearly but little atomic number contrast between the TiO and Sr columns. The HAADF image shows the strongest z-contrast difference between the metal containing columns but overall image signal-noise is poorer due to the large inner collection angle. The MAADF image offers a good compromise between composition information and image SNR.

PACBED patterns show increasing strength of Kikuchi bands with increasing wedge thickness, while column averaged scattering profiles (right) for constant thickness show increased high-angle scattering for the heavier Sr columns compared with TiO and O [1].

Nanoparticle Dark-field Optimisation

Precious metal nanoparticles are used widely in catalysis. Improving their design and performance requires high resolution imaging, but their small size makes them incredibly sensitive to electron beam damage. Using a pixelated detector allows for every scattered electron to be recorded with 100% efficiency and for the incoming beam current to be reduced.

Figure 4 shows an example detector lane image exhibiting single electron sensitivity; the detector sensitivity is so great a beam-blanker was sued here to improve the dynamic range in the dark-field regime. After reducing the electron dose, no sample damage was observed and sample and instrument stability was sufficient to produce an atomic resolution image of the nanoparticle supported only on amorphous carbon black (Figure 5).

Having acquired the 4D data-block of detector images at every probe position, the data were reshaped into a three dimensional volume of x-y and 'scattered intensity as a function of angle'. This three-dimensional volume can then be treated similarly to a spectrum image and inspected for optimised detector angles to reveal certain features [4].

Integrating the whole dark-field region gives a high signal-noise ADF image (Figure 5 left), but inspecting the low and medium angle scattering reveals detail within the twinned region at the left edge of the particle.

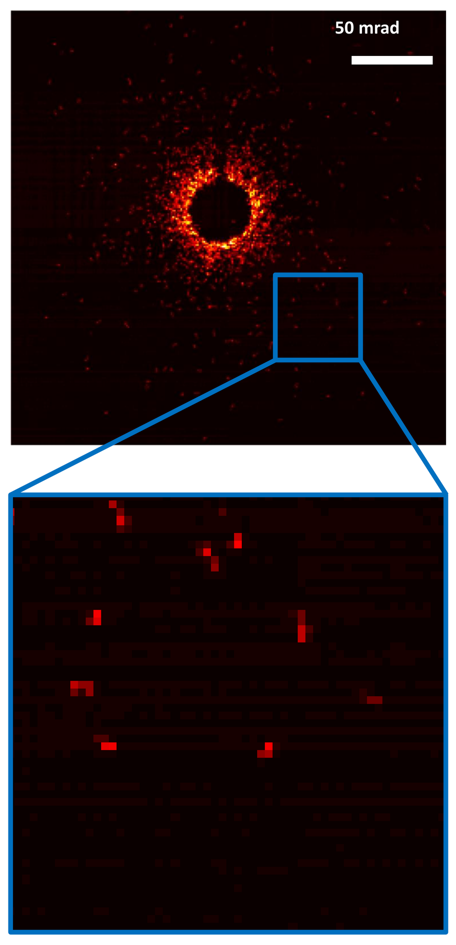

Figure 4. *Example detector image with 264x264 pixels. A beam-blanker was used to shield the camera from the BF disk. Enlargement shows the sensitivity of the camera t individual electron scattering events.*

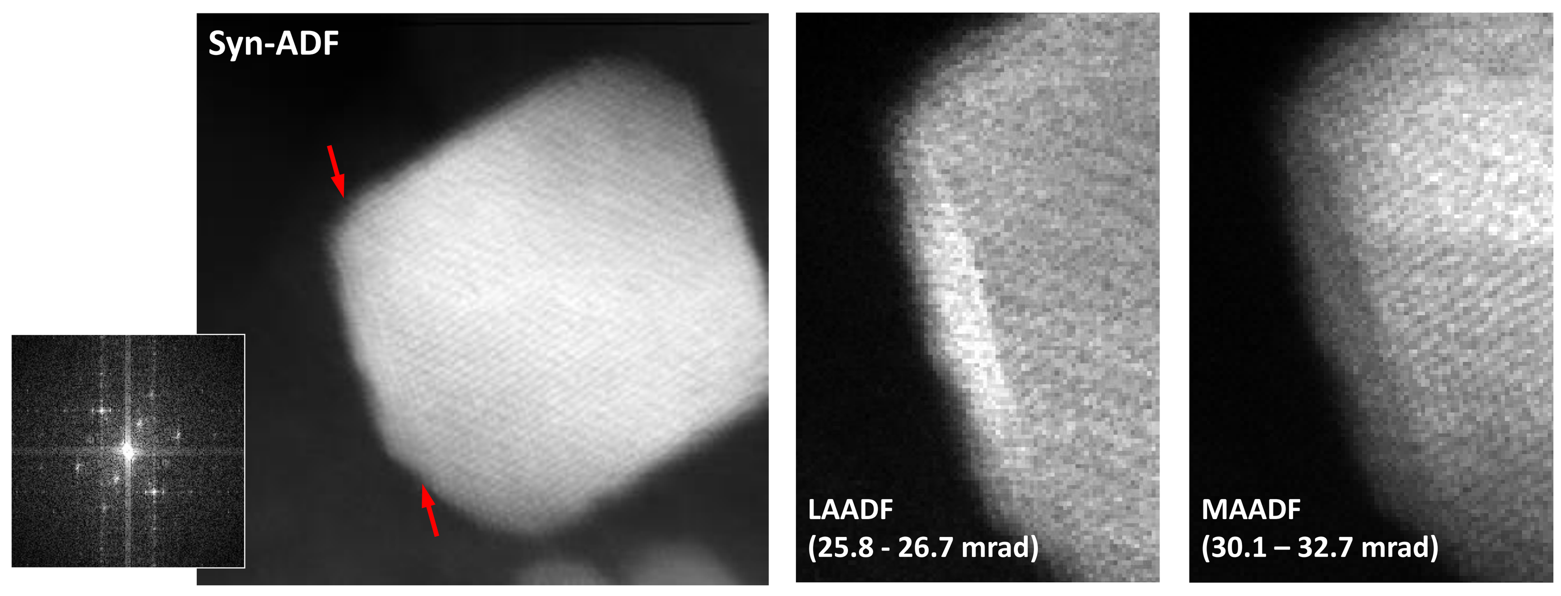

Figure 5. *Left: Atomic resolution synthetic-ADF image of PtCo nanoparticle formed using the whole dark-field regime. The red arrows indicate the position of a twin boundary; the inset FT shows superlattice spots from the ordering of the alloy. Right: Low-angle and medium-angle synthetic dark-field images where the surface layer appears first bright, then dark.*

Conclusions

Recording all the electrons scattered during STEM imaging on a pixelated camera yields a highly sensitive and rich dataset. This dataset can be analysed offline from the microscope using virtual detectors optimised to deliver the peak SNR for a given imaging mode. Additional data can be extracted about sample thickness from PACBED patterns or about sample composition from scattering curves such as those in Figure 3.

Operating the camera in an electron counting mode delivers single electron sensitivity (Figure 4) which allows maximally efficient dark-field STEM to be performed. This is especially useful for imaging fragile beam-sensitive materials such as nanoparticles.

References

1) K. Kimoto and K. Ishizuka, "Spatially resolved diffractometry with atomic-column resolution.," *Ultramicroscopy*, **111,**, p. 1111–6 (2011).
2) N. Shibata et al. "New area detector for atomic-resolution scanning transmission electron microscopy," *J. Electron Microsc.* , **59**, p. 473–479 (2010).
3) T. J. Pennycook et al. "Efficient phase contrast imaging in STEM using a pixelated detector: Part 1," *Ultramicroscopy*, **151**, p. 160–167 (2015).
4) A. De Backer et al. "Optimal experimental design for nano-particle atom-counting from high-resolution STEM images," *Ultramic.*, **151**, p. 46–55 (2015).

Acknowledgments

The authors would like to acknowledge ESTEEM2 (EU-FP7 grant agreement 312483) and EPSRC grant EP/M010708/1 for financially supporting this work and Johnson Matthey for the sample used in Figure 5.

* lewys.jones@materials.ox.ac.uk Copies of this poster are available online at: **www.lewysjones.com**